DOI: 10.1002/ejic.200600616

Synthesis and Structural Characterization of a Series of Carboxylic Acid Modified Cerium(III) Alkoxides

Timothy J. Boyle,*[a] Louis J. Tribby,[a] and Scott D. Bunge[a]

Keywords: Metal alkoxides / Cerium alkoxides / Carboxylate ligands / Chelates

A series of cerium alkoxides were synthesized from the reaction of $Ce\{N[Si(CH_3)_3]_2\}_3$ and the appropriate alcohol: neopentyl alcohol [$H–OCH_2C(CH_3)_3$ = H-ONep], *tert*-butyl alcohol [$H–OC(CH_3)_3$ = H-O*t*Bu], *o*-(*tert*-butyl)phenol {$H–OC_6H_4[C(CH_3)_3]$-2 = H-*o*BP}, 2,6-dimethylphenol [$H–OC_6H_3(CH_3)_2$-2,6 = H-DMP], 2,6-diisopropylphenol {$H–OC_6H_3[CH(CH_3)_2]_2$-2,6 = H-DIP}, 2,6-di-*tert*-butylphenol {$H–OC_6H_3[C(CH_3)_3]_2$-2,6 = H-DBP}, or 2,6-diphenylphenol [$H–OC_6H_3(C_6H_5)_2$-2,6 = H-DPP] using toluene (tol), tetrahydrofuran (THF) or pyridine (py). The precursors were characterized as $[Ce(\mu\text{-ONep})_2(ONep)]_4$ (**1**), $Ce_4(\mu_3\text{-O}t\text{Bu})_3(\mu\text{-O}t\text{Bu})_4(O t\text{Bu})_5$ (**2**), $Ce_3(\mu_3\text{-O}t\text{Bu})_3(\mu\text{-O}t\text{Bu})_3(O t\text{Bu})_3(\text{H-O}t\text{Bu})_2$ (**2a**), $Ce(o\text{BP})_3(THF)_3$ (**3**), $[Ce(\mu\text{-DMP})(DMP)_2(solv)_2]_2$ [solv = THF (**4**) and py (**4a**)], $Ce(DIP)_3(THF)_3$ (**5**), $Ce(DPP)_3(THF)_2$ (**6**). Once isolated, several of these species were further reacted with a series of sterically varied carboxylic acid modifiers including isobutyric acid [$H–O_2CCH(CH_3)_2$ = H-OPc] and trimethylacetic acid [$H–O_2CC(CH_3)_3$ = H-OBc]. The products were isolated as $[Ce(OR)(\mu\text{-ORc})(\mu_c\text{-ORc})(py)]_2$ [OR = *o*BP, OBc: **7**; DMP, OPc: **8**; DMP, OBc: **9**; DIP, OPc: **10**]. These compounds were identified by single-crystal X-ray diffraction and powder XRD analyses. Several novel structure types are added to the cerium alkoxide family of compounds.

Introduction

The role of metal alkoxide [$M(OR)_x$] precursors in ceramic materials synthetic routes such as, chemical solution (or the so-called "sol-gel"), metal organic chemical vapor deposition (MOCVD), or emerging nanoparticle synthetic methods have continued to expand. The growth is mainly due to their commercial availability, low crystallization temperatures, high solubility, high volatility, and other physical properties. In addition, these compounds are easily modified through the manipulation of their ligand set which allows for optimization of the final materials properties without increasing the complexity of the processing conditions. Typically, tailoring hydrolysis and condensation pathways of the $M(OR)_x$ precursors is of interest and accomplished by introducing a variety of ligands, including carboxylic acids (H–ORc). We have previously explored the structures obtained for group 4 alkoxides, modified with a series of H–ORc reagents, including: formic acid ($H–O_2CH$ = H-OFc), acetic acid ($H–O_2CCH_3$ = H-OAc), isobutyric acid [$H–O_2CCH(CH_3)_2$ = H-OPc], trimethylacetic acid [$H–O_2CC(CH_3)_3$ = H-OBc], or *tert*-butylacetic acid [$H–O_2CCH_2C(CH_3)_3$ = H-ONc], in an effort to understand how structure affects the final densification of thin films.[1,2] A number of general constructs were isolated for these systems but the partially hydrolyzed smaller trinuclear species proved to be the most useful for the generation of highly dense TiO_2 films and simple dinuclear species for ZrO_2 thin films.[1,2]

Recently, we have become interested in thin films of cerium oxide (CeO_x) as an anticorrosion material. In addition, CeO_x has demonstrated a wide variety of other applications, such as barrier layers,[3–5] counter electrodes for electrochromic glasses,[6] catalysts,[7–11] electrolytes for solid oxide fuel cells,[12–14] polishing agents for soft and hard optical glasses,[15,16] and numerous other applications. Due to the widespread use of CeO_x, it is surprising that only a few structurally characterized cerium alkoxides [$Ce(OR)_3$] have been reported in the literature,[17–29] and no systematic studies were possible from this eclectic mix of potential precursors. Because it is critical to know the structure of the precursor to be able to optimize the properties of the final CeO_x materials, it was necessary to develop a family of well-characterized, systematically structurally diverse $Ce(OR)_3$ precursors. Understanding the structural changes available for these precursors is critical prior to generating tailored-property CeO_x thin films.

Therefore, we undertook the synthesis and characterization of a series of $Ce(OR)_3$ that would fill in several gaps in the alkyl and aryl oxide derivatives to develop a systematic family of structurally characterized $Ce(OR)_3$ complexes which could be used to explore tailored materials. An alcohol amide metathesis reaction pathway was selected to synthesize these compounds [Equation (1)] in toluene (tol),

[a] Sandia National Laboratories, Advanced Materials Laboratory, 1001 University Boulevard SE, Albuquerque, New Mexico, 87105, USA
Fax: +1-505-272-7336
E-mail: tjboyle@Sandia.gov

tetrahydrofuran (THF), or pyridine (py). The products were identified as: $[Ce(\mu\text{-}ONep)_2(ONep)]_4$ where ONep = $OCH_2C(CH_3)_3$ (**1**), $Ce_4(\mu_3\text{-}OtBu)_3(\mu\text{-}OtBu)_4(OtBu)_5$ (**2**), $Ce_3(\mu_3\text{-}OtBu)_3(\mu\text{-}OtBu)_3(OtBu)_3(H\text{-}OtBu)_2$ (**2a**), where $OtBu = OC(CH_3)_3$, $Ce(oBP)_3(THF)_3$ {**3**, *o*BP = OC_6H_4-[$C(CH_3)_3$]-2}, $[Ce(\mu\text{-}DMP)(DMP)_2(solv)]_2$ [DMP = $OC_6H_3(CH_3)_2$-2,6, solv = THF (**4**); solv = py (**4a**)], $Ce(DIP)_3(THF)_3$ [**5**, DIP = $OC_6H_3[CH(CH_3)_2]_2$-2,6], and $Ce(DPP)_3(THF)_3$ [**6**, DPP = $OC_6H_3(C_6H_5)_2$-2,6]. Compounds **1**–**5** were further reacted with a series of sterically varied H–ORc modifiers and their products identified as: $[Ce(OR)(\mu\text{-}ORc)(\mu_c\text{-}ORc)(py)]_2$ [OR = *o*BP, OBc (**7**); DMP, OPc (**8**); DMP, OBc (**9**); DIP, OPc (**10**), py = pyridine; μ = bridging; μ_c = chelating bridge]. The synthesis, characterization, and crystal structures of **1**–**10** are discussed below.

$$Ce(NR_2)_3 + 3\ H\text{–}OR \rightarrow Ce(OR)_3 + 3\ H\text{–}NR_2 \quad (1)$$

Results and Discussion

As mentioned previously, we are interested in understanding the structural types available from simple OR- and ORc-modified Ce-based compounds prior to generating tailor-made CeO_x thin films. Only a limited number of X-ray crystallographically characterized $Ce(OR)_3$ species have been reported: $[Ce(\mu\text{-}OiPr)(OiPr)_3(H\text{–}OiPr)]_2$ [O*i*Pr = $OCH(CH_3)_2$],[27,28] $Ce_4(\mu_4\text{-}O)(\mu_3\text{-}OiPr)_2(\mu\text{-}OiPr)_4(OiPr)_8$,[24,29] $Ce_3(\mu_3\text{-}OtBu)_2(\mu\text{-}OtBu)_3(OtBu)_5(NO_3)$,[20] $[Ce(\mu\text{-}OR)(OR)_2]_2$ where OR = O*t*Bu[23] or $OCH(tBu)_2$,[26] $Ce[OC(tBu)_3]_3(CNtBu)_2$,[22] $[Ce\{OCH(tBu)_2\}_3(\mu\text{-}DMAE)]_2$ [DMAE = $Me_2N\text{–}C_2H_4\text{–}NMe\text{–}C_2H_4\text{–}O^-$],[21] and $[Ce\{OC(tBu)_3\}_3]_2(OC_6H_4O)$.[23] In contrast, significantly fewer aryl oxide derivatives have been isolated, including $Ce[OC_6H_3(tBu)_2]_3$,[25] $Ce[OC_6H_3(tBu)_2]_3(CNtBu)$,[25] and $Ce[OC_6H_3(C_6H_5)_2]_3$.[17] It is of note that other Ce-containing species are available with fluorinated ligands, siloxide ligands,[19] or the inclusion of other metals.[30,31]

This nonsystematic family of compounds does not lend insight into the possible structure types available for CeO_x precursors and thus necessitated the controlled synthesis of a series of $Ce(OR)_3$. Initial attempts focused on the aryl oxide ligands due to the dearth of structures available, the ease with which steric bulk can be introduced in the *ortho* positions, and our previous success using these ligands to produce high-quality thin films. We were also interested in several sterically demanding alkyl derivatives ONep and O*t*Bu due to our previous success using these ligands for materials synthesis and their lack of availability in the literature as homoleptic precursors.[20]

Cerium Alkoxides

Several routes to these $Ce(OR)_3$ were considered prior to initiating this investigation. The first attempts were made using a liquid ammonia route wherein $CeCl_3$ was added to Na^0 dissolved in NH_3(l) at –78 °C followed by addition of H-DIP in toluene. Crystallization of the hexanes-soluble fraction of this reaction mixture yielded $[Ce(\mu\text{-}DIP)(DIP)_2]_2$. Unfortunately, when altering the pendant chain to an alkyl group, Na contamination was observed.[32] This prevented us from using a standard route to the family of $Ce(OR)_3$ that we were interested in isolating. It was therefore necessary to adjusted our synthetic strategy, and we switched to an amide alcohol metathesis route [Equation (1)] based on our previous success with this route.[32] It is critical for the synthesis of these compounds that a very pure $Ce(NR_2)_3$ be used, which was obtained by repeated sublimations and crystallizations.

Synthesis

For each reaction, the $Ce(NR_2)_3$ was dissolved in toluene yielding a pale yellow solution. Upon addition of the desired alcohol, the reaction mixture was warmed slightly and turned clear with no precipitates observed for any of these samples. Crystals were isolated by drastically reducing the volume of the reaction and cooling the mixture to –25 °C. FTIR data indicates for each sample that the crystals did not possess any amide ligands and that the alcohols had fully reacted. Solution-state NMR could not be obtained due to the paramagnetic nature of the Ce^{III} species isolated, therefore, it was necessary to obtain single-crystal X-ray structures to identify these compounds. The results of these experiments are shown in Figure 1 to Figure 12 for **1**–**10**, respectively.

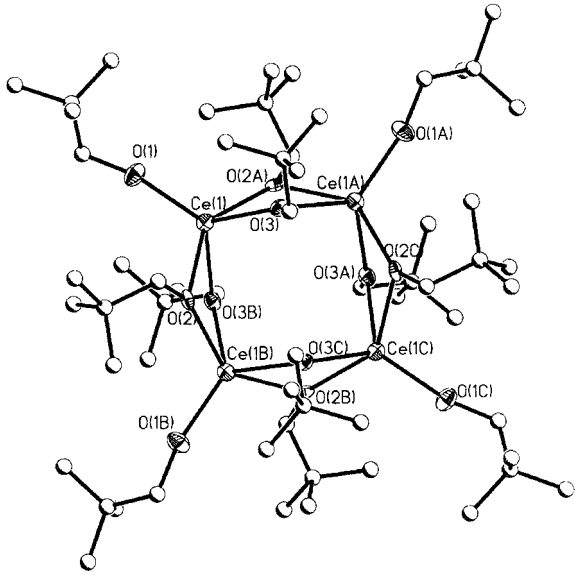

Figure 1. Structure plot of **1**. Thermal ellipsoids of heavy atoms drawn at 30% level. Carbon atoms are drawn as ball and stick for clarity.

Crystal Structures

For **1**, the least sterically hindering ONep ligand led to the formation of a tetranuclear species, which is identical

to what was reported for the all of the lanthanide ONep derivative, see Figure 1.[32–34] The central core consists of four Ce metal centers arranged in a square, interconnected by four bridging μ-ONep ligands and one terminal ONep ligand per metal. Each of the Ce cations is five-coordinated adopting a square-base-pyramidal (SBP) geometry. As reported for the other $[Ln(ONep)_3]_4$ species,[32–34] there is significant H-bonding interaction noted for this compound.

Increasing the steric demands from the ONep to the O*t*Bu ligand, under stoichiometric conditions, led to the isolation of another tetranuclear species **2** (Figure 2). For **2**, the four octahedrally bound (O_h) metals are again arranged in a square linked by μ-O*t*Bu ligands; however, in contrast to **1**, three μ_3-O*t*Bu link the metal centers: Ce(1), Ce(2), and Ce(3) through the use two of the μ_3-O*t*Bu while the remaining μ_3-O*t*Bu bridges Ce(1), Ce(2), and Ce(4). To complete the O_h geometry, Ce(1), Ce(2) and Ce(3) bind one terminal O*t*Bu ligand each and Ce(4) coordinates two ligands. This structure is similar to what was observed for $Ce_4(\mu_4\text{-}O)[\mu_3\text{-}OCH(CH_3)_2]_2[\mu\text{-}OCH(CH_3)_2]_4[OCH(CH_3)_2]_8$,[24,29] which uses an oxo ligand to achieve this structure; however, this is the first structural arrangement of this type noted for homoleptic $Ln(OR)_3$. When excess H-O*t*Bu is used, a centrosymmetric trinuclear species **2a** (Figure 3), similar to other lanthanide alkoxides is isolated in the presence of Lewis base solvents. For **2a**, each Ce is bound by two μ_3-O*t*Bu, two μ-O*t*Bu and two terminal O*t*Bu ligands adopting a distorted trigonal bipyramidal (TBP) arrangement. By charge balance, two of these ligands must be protonated, as is commonly noted for metal alkoxides.[35,36] The increased steric bulk of the bound Lewis base H-O*t*Bu does not allow for large clusters to form. The mixed charge NO_3 derivative $Ce_3[\mu_3\text{-}OC(CH_3)_3]_2[\mu\text{-}OC(CH_3)_3]_3[OC(CH_3)_3]_5(NO_3)$,[20] and other solvated $Ln(OR)_3$ are known to adopt this structure as well.[37] It is interesting to note that the primary alcohol H-ONep is often considered to be less sterically hindering than the tertiary H-O*t*Bu, but in this system, the ONep-ligated species yields Ce metal centers with a lower coordination number. One explanation for this phenomenon may be the significantly greater cone angle swept out by the ONep ligand as compared to that of the O*t*Bu ligand.

Because only slight changes in the structure were noted for the pure alkoxides isolated above, in comparison to the literature species, further probing of the influence of sterics on the structure of these compounds led to an investigation of aryl oxide derivatives. For this system, it was necessary to use Lewis base solvents to maintain solubility. Using an asymmetrically substituted aryl oxide (*o*BP) wherein the steric bulk of one of the *ortho* sites is increased to a *tert*-butyl group, the first mono-substituted alkyl phenoxide lanthanide alkoxide complex was isolated as **3** (Figure 4). It is of note that several lanthanide alkali metal double alkoxides with 4-methylphenoxides[38,39] have been isolated previously.[39,40] The *tert*-butyl groups of the *o*BP ligands all point away from the metal center allowing the coordination of three THF solvent molecules forming a *fac* O_h metal center.

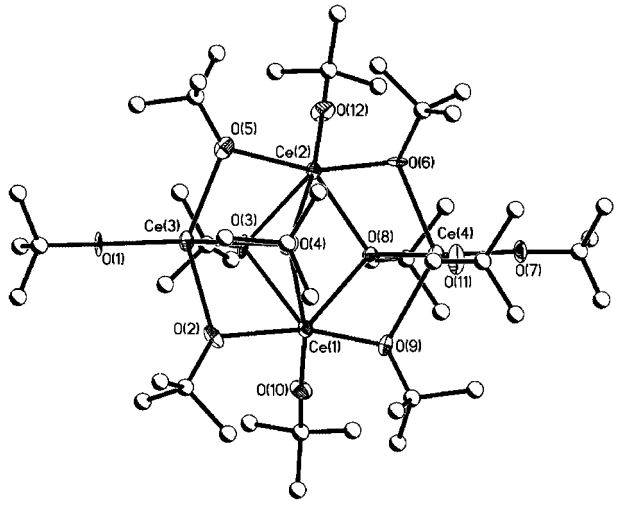

Figure 2. Structure plot of **2**. Thermal ellipsoids of heavy atoms drawn at 30% level. Carbon atoms are drawn as ball and stick for clarity.

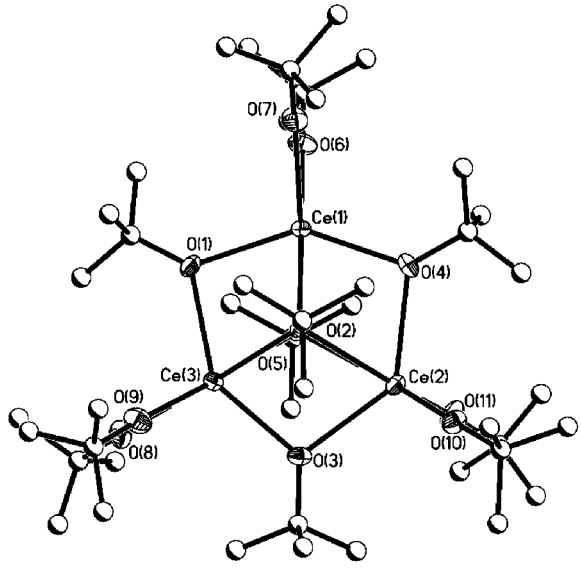

Figure 3. Structure plot of **2a**. Thermal ellipsoids of heavy atoms drawn at 30% level. Carbon atoms are drawn as ball and stick for clarity.

Systematically increasing the steric bulk by placing a methyl group in each *ortho* position, surprisingly led to the isolation of the dinuclear species **4**, shown in Figure 5. Each of the Ce metal centers adopts a distorted O_h geometry by binding two μ-DMP, two terminal DMP, and two THF solvent molecules in the axial position. It was thought that the delicate balance between steric bulk and coordination strength of the solvent allowed a monomer to form as noted for **3** vs. the dinuclear for **4**. Therefore, a stronger Lewis base was used in the synthesis to see if **4** could be converted to a mononuclear species. Surprisingly, switching to py, lead to the isolation of **4a** which adopts an identical dinuclear structure as observed for **4** but the THF ligands are replaced by py ligands (Figure 6). This is the first py adduct of $Ce(OR)_3$ reported to date. Compounds **4** and **4a** are

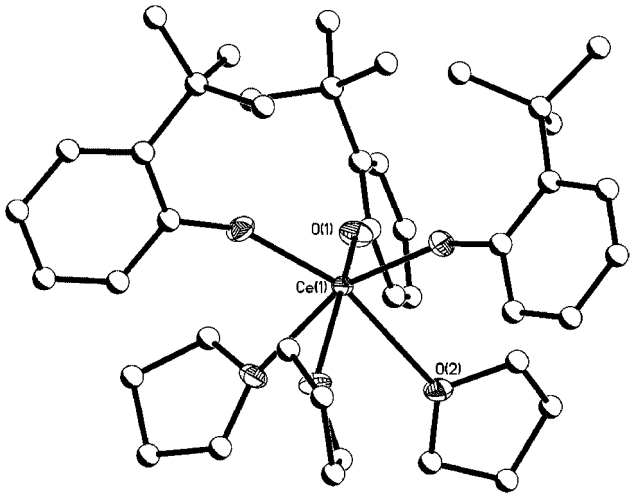

Figure 4. Structure plot of 3. Thermal ellipsoids of heavy atoms drawn at 30% level. Carbon atoms are drawn as ball and stick for clarity.

analogous to $[Y(\mu\text{-DMP})(DMP)_2(THF)]_2$ structure previously reported.[41]

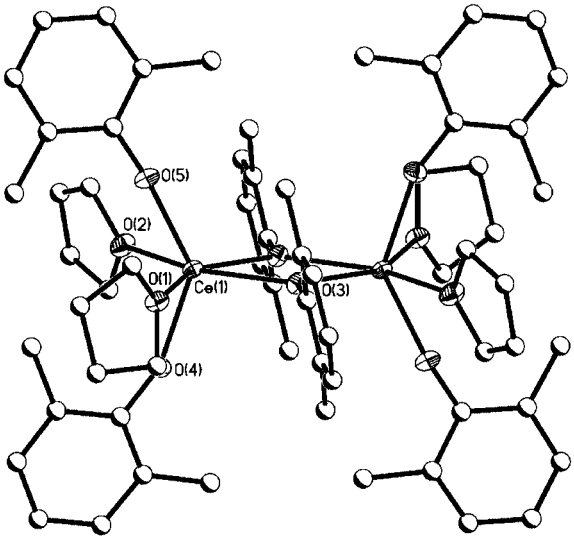

Figure 5. Structure plot of **3a**. Thermal ellipsoids of heavy atoms drawn at 30% level. Carbon atoms are drawn as ball and stick for clarity.

For compound **5** shown in Figure 7, the further increase in steric bulk of the *ortho* positions to isopropyl groups coupled with the use of Lewis base solvents, led to the formation of a monomer. The Ce metal center is O_h bound by three DIP and three THF ligands in a *fac* arrangement, as noted for the *o*BP ligated species and numerous literature reports of solvated lanthanide monomers.[40] In comparison, the larger La cation only used two solvent molecules to complete its coordination sphere for the same ligand set;[42] however, smaller cations have also been found to yield trisolvated species such as $Sm(DIP)_3(THF)_3$.[43] Therefore, the number of solvent molecules coordinated can not be directly related to the size of the cations employed. A similar mononuclear structural arrangement was observed for the DPP (**6**, Figure 8) ligated compound; however, for **6** only two THF molecules are present. The previously reported DPP derivative was also a monomer but had π interactions from the *ortho* phenyl groups,[17–29] therefore, the addition of coordinated solvent noted for **6** is not unexpected. For the $Ln(DPP)_3(THF)_2$ Ln = La,[42,44] Nd,[42,44] Yb[45,46] complexes, the large *trans* effect of the OAr and the THF ligands was also observed for **6**.

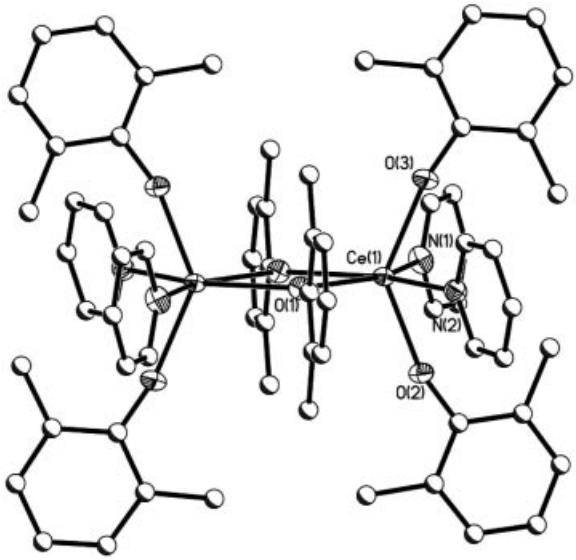

Figure 6. Structure plot of **4**. Thermal ellipsoids of heavy atoms drawn at 30% level. Carbon atoms are drawn as ball and stick for clarity.

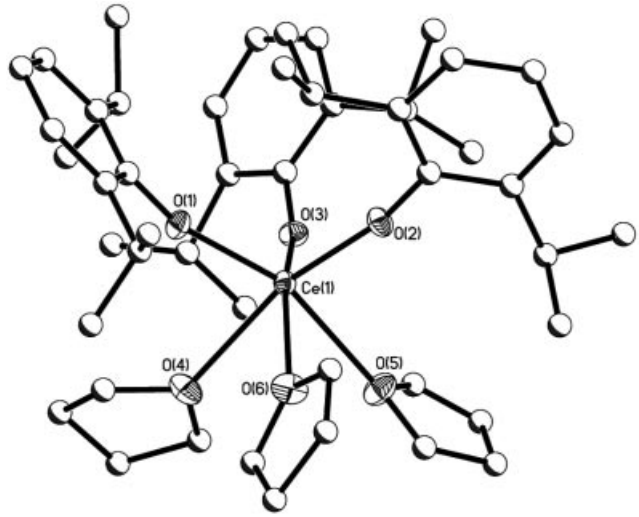

Figure 7. Structure plot of **5**. Thermal ellipsoids of heavy atoms drawn at 30% level. Carbon atoms are drawn as ball and stick for clarity.

The bond lengths and angles of this family of Ce^{III} alkoxides, **1**–**6**, are consistent with those of previously reported $Ce(OR)_3$.[17–29,32–34,47,48] For **1**, as the second largest cation

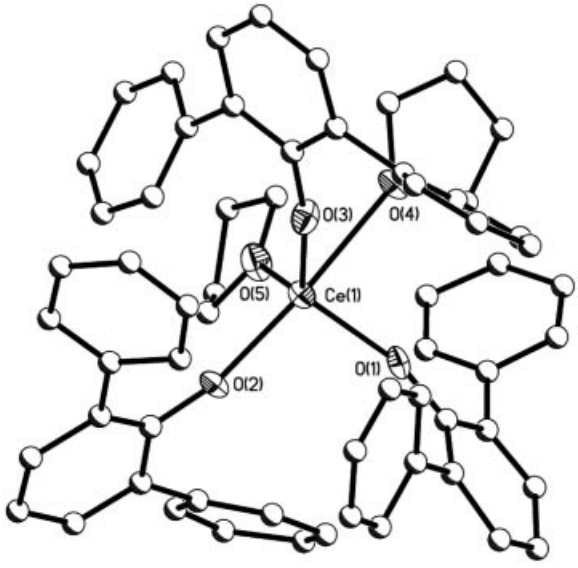

Figure 8. Structure plot of **6**. Thermal ellipsoids of heavy atoms drawn at 30% level. Carbon atoms are drawn as ball and stick for clarity.

in the ONep family of $[Ln(\mu\text{-}ONep)_2(ONep)]_4$ it falls on the long end of the Ln···Ln separations which systematically decrease from 3.86 to 3.28 Å. Terminal Ln–O distances of 2.14 Å for Ce fall within the range 2.16 Å (La, average value) to 1.89 Å (Sc) with an overall average distance of 2.06 Å. Ce is the second largest cation so obviously the Ce–O distance falls at the longer end of the observed bond lengths.

The O*t*Bu derivative **2** was found to adopt a novel structure type and no acceptable models were available for structural comparisons; however, the Ce(III/IV) oxo isopropoxide[24,29] was the closest in terms of connectivity and composition. The average terminal Ce–OR distances of 2.12, Ce(μ-OR) of 2.31, and Ce(μ_3-OR) of 2.47 Å were *not* found to be in agreement with **2** [2.24 (terminal), 2.44 (μ) Å]. This is most likely a reflection of the varied oxidation state and oxo species for the Ce(III/IV) oxo isopropoxide[24,29] complex vs. the Ce^{III} alkoxide for **2**. There is also a trinuclear Ce(III/IV) O*t*Bu derivative structurally consistent with **2a**; however, the average Ce–OR, Ce(μ-OR), and Ce(μ_3-OR) distances of 2.08, 2.37, and 2.52 Å, respectively, are *not* in agreement with **2a** [2.23 (terminal) and 2.45 (μ) Å]. These differences are not surprising due to the mixed valent Ce(III/IV) species. Because the lanthanides systematically vary in cation size due to the lanthanide contraction, it is valid to use the isostructural La derivatives for metrical comparisons. In general, the bond lengths and angles of **2a** were found to be in agreement with $La_3(O\mathit{t}Bu)_9(H\text{-}O\mathit{t}Bu)_2$.[49] For example, the average μ_3-OR–Ln distances are 2.55 Å for **2a** and 2.57 Å for La.

The dinuclear species **4** and **4a** have average Ce–OR and Ce(μ-OR) distances of 2.25 and 2.45 Å, respectively; **5** has an average Ce–OR distance of 2.22 Å. The dinuclear $O\mathit{t}Bu/OC\mathit{t}Bu_3$,[23] O*i*Pr,[27,28] $OC(CH_3)_2(\mathit{i}Pr)$,[48] and $OC(H)(\mathit{t}Bu)_2$[26] have average distances of 2.14 Å for Ce–OR and 2.36 Å for Ce(μ-OR). The monomeric species that are solvated[17,25,48] also have a similar average Ce–OR distance of 2.17 Å. The mononuclear solvated **6** was found to be in agreement with the metrical data reported for the unsolvated but π-bound DPP;[17–29] the average Ce–OR distances were 2.21 Å for **5** and 2.24 Å for **6**.

Carboxylic Acid Modified Cerium Alkoxides

It was of interest to add more protective groups to the metal center to reduce the sensitivity to hydrolysis as well as introduce new constructs for $Ce(OR)_3$. This was undertaken using H-ORc. Previous studies[1,50,51] have shown that substantial changes in the rate of hydrolysis and condensation can be wrought through the introduction of H-ORc modifiers both through esterification oxolation pathways and the steric hindrance introduced by the bidentate nature of the ORc ligand. It is of note that the μ- and μ_c-ORc ligands (also referred to as bidentate and tridentate, respectively) have been observed in a variety of lanthanide carboxylate systems wherein over 1500 structures have been identified revealing a variety of binding modes available for Ln–ORc species.[40] A further search of the literature reveals many Ce–ORc compounds have been structurally characterized but the majority of these are the homoleptic species.[52–62] with no structurally characterized carboxylate-modified alkoxide compounds available.

Synthesis

Therefore, we investigated the modification of the $Ce(OR)_3$ isolated above with a series of sterically varied carboxylic acids. In general, the compounds were dissolved in py and then added to a stirring solution of the carboxylic acid dissolved in py. No precipitates were observed. Because the Ce^{III} metal center is paramagnetic, solution identification of these compounds by NMR methods was not possible. Further, the volatility of the bound solvent prevents clean identification of the bulk powder by thermal elemental analyses. Therefore, while we have isolated numerous powders from these reactions, only those that were structurally characterized will be discussed below.

After numerous attempts, only the OAr–ORc modified species were structurally characterized. This phenomenon was mainly attributed to the ability of the steric bulk of the aryl oxide to prevent larger less soluble precursors to form. This is clearly illustrated by the larger oligomers observed for both the ONep and O*t*Bu ligated species **1**–**2** in comparison to the OAr derivatives **3**–**5**.

X-ray Crystal Structure

Figure 9 shows the structure plot of **7**, the OBc-modified species of **3** that was isolated as the substituted dinuclear species. The OBc ligands have replaced two of the *o*BP ligands and bridge between the metal centers in two coordination modes: bridging (μ-ORc) and bridging chelating (μ_c-

ORc) modes. By binding two py and the original *o*BP ligands, this forms eight-coordinate Ce metal centers forming a dodecahedron[63] arrangement. Independent of an increase in steric bulk of the pendant ORc chain, an identical core was observed for each of the various modified species [DMP/OPc **8** (Figure 10); DMP/OBc **9** (Figure 11), and DIP/OPc **10** (Figure 12)]. Interestingly, no esterification or redox behavior was noted for any of these reactions which is in stark contrast to the early transition metal ORc-modified compounds, wherein, esterification products were isolated for all but the most sterically hindering ligands.[1,2,64,65]

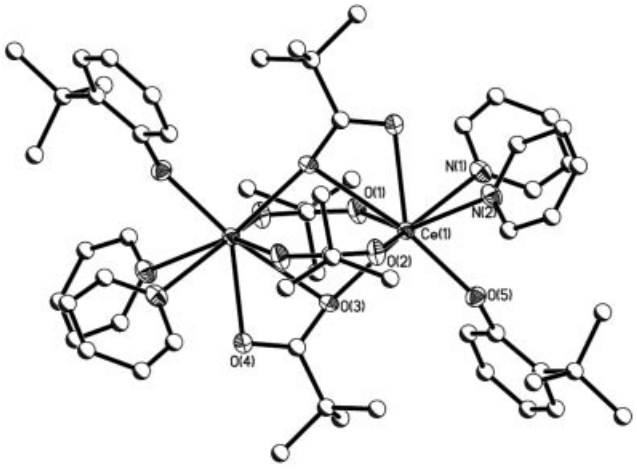

Figure 9. Structure plot of **7**. Thermal ellipsoids of heavy atoms drawn at 30% level. Carbon atoms are drawn as ball and stick for clarity.

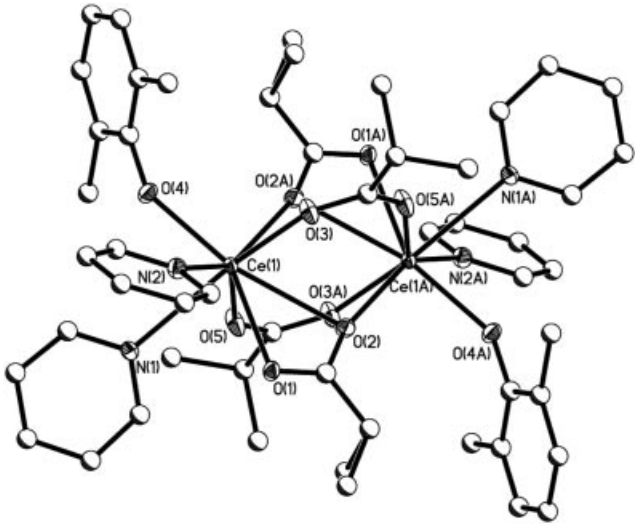

Figure 10. Structure plot of **8**. Thermal ellipsoids of heavy atoms drawn at 30% level. Carbon atoms are drawn as ball and stick for clarity.

The bond lengths and angles of the alkoxides[17–29,32–34,47,48] and the carboxylates moieties[52–62] are consistent with literature reports. The terminal distances of the aryl oxides are on the order of 2.24 to 2.27 Å and as noted above are within the expected range.[17–29,32,33,47,48] The bite angle of the μ_c-ORc in the literature[52–62] have

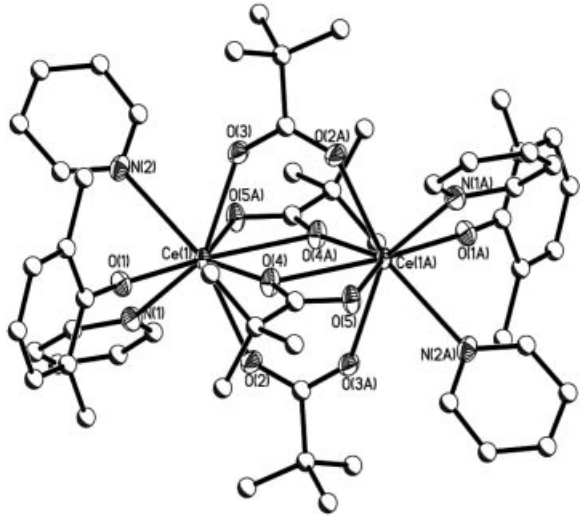

Figure 11. Structure plot of **9**. Thermal ellipsoids of heavy atoms drawn at 30% level. Carbon atoms are drawn as ball and stick for clarity.

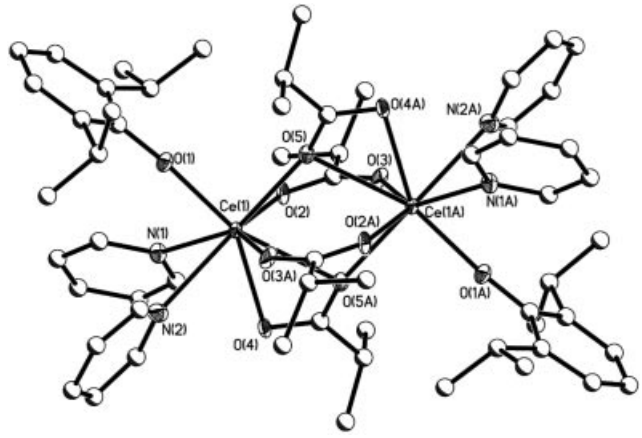

Figure 12. Structure plot of **10**. Thermal ellipsoids of heavy atoms drawn at 30% level. Carbon atoms are drawn as ball and stick for clarity.

values ranging from 116° to 128° with an average value of 120.7°. The angles noted for **7**–**10** (121.3°, 121.3°, 120.9°, 119.6°, respectively) fall within this range. The μ-ORc ligands are limited to a few species with a smaller bite angle range (119° to 126°) with an average value of 123.4°, which is similar to the average values noted for **7**–**10**: 123.8°, 125.2°, 124.9°, 125.6°, respectively.

Bulk Powder Characterization

In an effort to characterize the bulk powder, several analytical methods were investigated. Typically, solution NMR can be employed to elucidate purity; however, the paramagnetic nature of the Ce^{III} metal centers prevents obtaining any meaningful data by these techniques. Solid-state NMR spectroscopic data also proved inconclusive due to broad and numerous peaks expected for these structures. These phenomena were also attributed to the paramagnetic nature

of the Ce^{III} and packing disorders, because the ligands are not free to rotate in the solid state numerous peaks are often observed.

The elemental analyses of the bulk powders of **1**–**10**, in general, agree with the unsolvated compounds. Compound **4a** is a solvated species and the slight variation in the elemental analysis was attributed to either "trapped" and/or bound solvent. These conditions are often reported to cause variations from ideal conditions.[50,51,66,67] FTIR spectra of **1**–**10** revealed the presence of the appropriate stretches expected for the various alkoxide ligands and shifts of the ORc ligands consistent with them bound to a metal center. It is of note that there are some reports that indicate these compounds can undergo a reaction with KBr under high pressure, yielding spectra that may not reflect the actual species but a metathesis products instead.[68] However, these spectra are useful in terms of identifying the resultant products. Further investigations of these materials by TGA/DTA revealed that most samples did not show consistent weight losses or thermal behavior during processing. This is attributed to high reactivity with the ambient atmosphere as an artefact with our current experimental setup. This led to total weight losses that were rarely in agreement with the crystal structure. Due to the complexity of the above data, it is not possible to conclusively deduce the purity of the bulk powder and alternative methods were investigated.

Therefore, microXRD spectra were obtained on the $Ce(OR)_3$ bulk powders sealed in glass capillary tubes and compared to calculated patterns from the obtained single crystal structures. In general, the resulting spectra matched what was expected for the powder XRD patterns. Figure 13 and Figure 14 show the obtained microXRD results for **2a** and **6** and their general agreement with the theoretical spectrum (inset). The variations noted can be contributed to two factors (i) the calculated patterns generated from the crystal structure are based on a truly random powder and the crystals have preferential orientation and (ii) the powders are not solvated as are the crystal structures. Therefore, an exact match was not obtained; however, the powders do appear to agree to a significant degree with the calculated patterns.

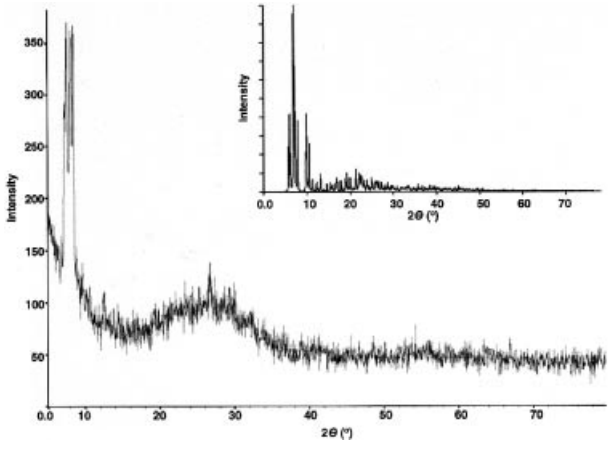

Figure 13. MicroXRD spectrum of **2a**. Inset is the calculated pattern.

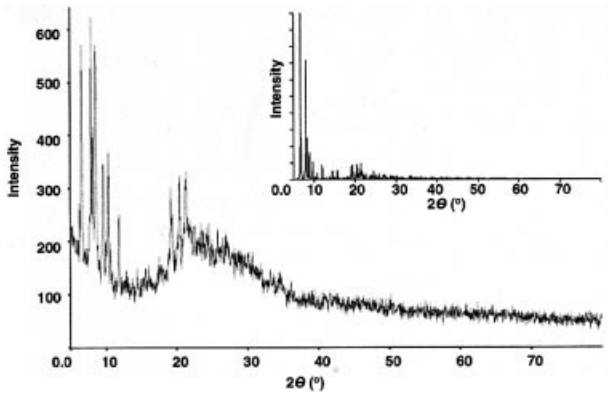

Figure 14. MicroXRD spectrum of **6**. Inset is the calculated pattern.

Summary and Conclusion

A family of Ce^{III} alkoxides were isolated through an alcohol–amide exchange reaction pathway. In general, as the steric bulk of the pendant alkoxy moiety increased and the presence of a Lewis base, the nuclearity of the molecule decreased. Species ranged from tetra- to mono-nuclear species with several novel solvents as ligands and arrangements noted for this family of compounds. The successful modification of the aryl oxide complexes led to the first alkoxy carboxylate structures isolated for Ce. These compounds were identified as dinuclear species with μ-ORc and μ_c-ORc ligands. The change in steric bulk of the OAr or the ORc ligand had no effect on the final structure. Interestingly, none of the ORc–$Ce(OR)_3$ possessed an oxo species indicating that esterification did not occur. These compounds are being investigated as precursors to CeO_x nanoparticles and thin films wherein the ligand set controls the structure and reactivity, which imparts control to the final properties of these CeO_x materials.

Experimental Section

All reactions were performed under a dry, inert atmosphere using standard Schlenk line and glovebox techniques. The following chemicals were used as received (Aldrich): $CeBr_3$, $KN[Si(CH_3)_3]_2$ (KNR_2), H-ONep, H-O*t*Bu, H-DMP, H-DIP, H-DPP, H-*o*BP, H-OPc, H-OBc, and H-ONc. H-OFc and H-OAc were dried according to literature preparative methods.[69] All solvents were used as received in anhydrous (Sure/Seal™) bottles. $Ce(NR_2)_3$ [where R = $Si(CH_3)_3$] was isolated from the reaction of $CeBr_3$ and 3 equiv. of KNR_2.[35,36] FT-IR spectroscopic data were obtained with a Bruker Vector 22 spectrometer using KBr pellets pressed under argon and handled under flowing nitrogen. Elemental analyses were performed with a Perkin–Elmer 2400 CHN-S/O elemental analyzer. Micro powder X-ray diffraction was performed with several samples that were prepared in a glass (Quartz) capillary and mounted vertically on an XYZ stage of a Bruker D8 Discover diffractometer

using Cu-K_α radiation (λ = 1.5406 Å). The X-ray beam was collimated to 1 mm size and scans are typically taken from 10 to 80 ° 2θ at 0.04 degree steps at 2 s per step. Diffraction scan interpretation was done using MDI, Inc. Jade 7 software.

General Alkoxide Synthesis: Due to the similarity of the synthesis of compounds **1**–**6**, a general description will be provided. The appropriate alcohol was dissolved in the solvent of choice and slowly added to a stirring solution of $Ce(NR_2)_3$ dissolved in the same solvent. The resulting solutions were stirred for 12 h and then the volume of the volatile material was drastically reduced by rotary evaporation. After this, the mixture was cooled to –25 °C until crystals formed.

$[Ce(\mu\text{-}ONep)_2(ONep)]_4$ (1): Used $Ce(NR_2)_3$ (0.60 g, 0.97 mmol), H-ONep (0.25 g, 2.9 mmol) in toluene (tol). Yield: 87% (0.34 g). FT-IR (KBr): $\tilde{\nu}$ = 2951 (w), 2864 (m), 2803 (m), 2687 (s), 1478 (m), 1460 (m), 1390 (s), 1358 (m), 1254 (s), 1215 (s), 1106 (w), 1059 (m), 1019 (m), 932 (s), 896 (s), 749 (s), 702 (s), 592 (m), 561 (s), 426 (s) cm^{-1}. $C_{60}H_{132}Ce_4O_{12}$ (1606.20): calcd C 44.87, H 8.28; found C 44.67, H 8.17.

$Ce_4(\mu_3\text{-}OtBu)_3(\mu\text{-}OtBu)_4(OtBu)_5$ (2): Used $Ce(NR_2)_3$ (0.61 g, 0.98 mmol), H-O*t*Bu (0.22 g, 3.0 mmol) in tol. Yield: 89% (0.32 g). FT-IR (KBr, cm^{-1}): $\tilde{\nu}$ = 2960 (w), 2865 (w), 2150 (s), 2120 (s), 1936 (s), 1848 (s) 1466 (w), 1356 (w), 1187 (w), 974 (w), 929 (w), 878 (w), 829 (w), 767 (w), 740 (w), 693 (s), 677 (s), 655 (s), 595 (m). $C_{48}H_{108}Ce_4O_{12}$ (1437.87): calcd C 40.09, H 7.57; found C 39.78, H 7.68.

$Ce_3(\mu_3\text{-}OtBu)_3(\mu\text{-}OtBu)_3(OtBu)_3(H\text{-}OtBu)_2$ (2a): Used $Ce(NR_2)_3$ (0.61 g, 0.98 mmol), H-O*t*Bu (0.29 g, 3.9 mmol) in tol. Yield: 90% (0.36 g). FT-IR (KBr, cm^{-1}): $\tilde{\nu}$ = 2965 (w), 2925 (w), 2865 (w), 1467 (m), 1370 (m), 1356 (w), 1020 (m), 968 (w), 927 (w), 878 (w), 768 (m), 759 (m), 740 (s), 511 (w), 488 (w). $C_{44}H_{101}Ce_3O_{11}$ (1226.65): calcd. C 43.08, H 8.30; found C 42.78, H 8.09.

$Ce(oBP)_3(THF)_3$ (3): Used $Ce(NR_2)_3$ (1.3 g, 2.9 mmol), H-*o*BP (0.91 g, 6.1 mmol) in tol. Yield: 92% (1.5 g). FT-IR (KBr, cm^{-1}): $\tilde{\nu}$ = 3056 (s), 2952 (m), 1587 (m), 1561 (m), 1478 (w), 1439 (w), 1301 (w), 1260 (w), 1217 (m), 1124 (s), 1088 (s), 1068 (s), 1047 (s), 1035 (s), 1003 (s), 868 (w), 823 (m), 748 (w), 703 (w), 597 (s). $C_{42}H_{63}CeO_6$ (804.09): calcd. C 62.74, H 7.90; found C 62.36, H 7.81.

$[Ce(\mu\text{-}DMP)(DMP)_2(THF)_2]_2$ (4): Used $Ce(NR_2)_3$ (0.22 g, 0.35 mmol), H-DMP (0.13 g, 1.10 mmol) in tetrahydrofuran (THF). Yield: 95% (0.22 g). FT-IR (KBr, cm^{-1}): $\tilde{\nu}$ = 2971 (s), 1591 (m), 1465 (m), 1425 (m), 1367 (s), 1269 (w), 1233 (w), 1211 (w), 1094 (m), 1068 (s), 1027 (m), 850 (w), 761 (m), 697 (m), 678 (s), 565 (s), 524 (s), 492 (s). $C_{64}H_{86}Ce_2O_{10}$ (1295.63): calcd. C 59.33, H 6.69; found C 59.16, H 7.05.

$[Ce(\mu\text{-}DMP)(DMP)_2(py)_2]_2$ (4a): $Ce(NR_2)_3$ (0.97 g, 1.6 mmol), H-DMP (0.58 g, 4.7 mmol) in tol and pyridine (py). Yield: 95% (0.98 g). FT-IR (KBr, cm^{-1}): $\tilde{\nu}$ = 3068 (m), 3049 (m), 3012 (m), 2964 (m), 2909 (s), 1596 (w), 1465 (w), 1442 (w), 1424 (w), 1270 (w), 1234 (w), 1210 (w), 1150 (s), 1092 (w), 1067 (m), 1035 (m), 1003 (m), 850 (w), 837 (w), 747 (w), 621 (m), 564 (s), 526 (m). $C_{68}H_{74}Ce_2N_4O_6$ (1323.61): calcd. C 61.70, H 5.64, N 4.23; found C 60.87, H 5.66, N 4.48.

$Ce(DIP)_3(THF)_3$ (5): Used $Ce(NR_2)_3$ (0.22 g, 0.36 mmol), H-DIP (0.19 g, 1.1 mmol) in tol and THF. Yield: 96% (0.22 g). FT-IR (KBr, cm^{-1}): $\tilde{\nu}$ = 3054 (s), 2958 (w), 2867 (m), 1586 (s), 1380 (s), 1357 (s), 1327 (m), 1264 (w), 1206 (m), 1095 (s), 1042 (m), 1021 (m), 885 (m), 855 (w), 796 (s), 752 (m), 687 (m), 561 (m). $C_{48}H_{75}CeO_6$ (888.25): calcd. C 64.91, H 8.51; for $C_{36}H_{51}CeO_3$ (without 3THF, 671.92): calcd. C 64.35, H 7.65; found C 63.96, H 8.04.

$Ce(DPP)_3(THF)_2$ (6): Used $Ce(NR_2)_3$ (0.24 g, 0.39 mmol), H-DPP (g, 1.2 mmol) in THF. Yield: 99% (0.39 g). FT-IR (KBr, cm^{-1}): $\tilde{\nu}$ = 3054 (m), 3027 (m), 2975 (m), 2874 (m), 1596 (w), 1581 (m), 1495 (w), 1453 (w), 1405 (w), 1307 (w), 1261 (w), 1176 (m), 1156 (s), 1086 (w), 1069 (w), 1025 (w), 914 (m), 856 (w), 803 (s), 702 (w), 626 (s), 600 (w). $C_{62}H_{55}CeO_5$ (1020.24): calcd. C 72.99, H 5.43; found C 72.64, H 5.79.

General Modified Alkoxide Synthesis: Due to the similarity of the synthesis of compounds **7**–**10**, a general description will be provided. To a stirring solution of the appropriate $Ce(OR)_3$ (**1**–**5**), 1 equiv. of the appropriate H-ORc was added. The reaction was stirred for 12 h and then the volatile portion was allowed to slowly evaporate until crystals formed.

$[Ce(oBP)(\mu\text{-}OBc)(\mu_c\text{-}OBc)(py)_2]_2$ (7): Used compound **3** (0.26 g, 0.32 mmol), H-OBc (0.066 g, 0.65 mmol) in py. Yield: 92% (0.20 g). FT-IR (KBr, cm^{-1}): $\tilde{\nu}$ = 2962 (m), 1524 (w), 1483 (w), 1459 (w), 1418 (w), 1375 (w), 1224 (m), 1032 (s), 897 (s), 802 (s), 601 (s), 540 (s). $C_{60}H_{82}Ce_2N_4O_{10}$ (1299.58): calcd. C 55.45, H 6.36, N 4.31; found C 55.19, H 6.81, N 4.01.

$[Ce(DMP)(\mu\text{-}OPc)(\mu_c\text{-}OPc)(py)_2]_2$ (8): Used compound **4** (0.28 g, 0.22 mmol), H-OPc (0.038 g, 0.43 mmol) in py. Yield: 37% (0.10 g). FT-IR (KBr, cm^{-1}): $\tilde{\nu}$ = 2968 (w), 2930 (m), 1581 (w), 1477 (w), 1422 (w), 1373 (m), 1359 (m), 1238 (m), 1217 (w), 1092 (w), 1035 (m), 1004 (m), 850 (w), 753 (w), 702 (w), 663 (s), 619 (m), 547 (m), 531 (m), 518 (m). $C_{52}H_{66}Ce_2N_4O_{10}$ (1187.37): calcd. C 52.60, H 5.60, N 4.71; found C 52.39, H 5.52, N 4.19.

$[Ce(DMP)(\mu\text{-}OBc)(\mu_c\text{-}OBc)(py)_2]_2$ (9): Used compound **4** (0.44 g, 0.34 mmol), H-OBc (0.069 g, 0.68 mmol) in py. Yield: 53% (0.22 g). FT-IR (KBr, cm^{-1}): $\tilde{\nu}$ = 3607 (s), 2961 (w), 2929 (w), 2871 (w), 1541 (w), 1483 (w), 1460 (w), 1420 (w), 1375 (w), 1361 (w), 1285 (m), 1263 (w), 1224 (w), 1090 (m), 1033 (m), 896 (w), 839 (m), 803 (m), 791 (m), 756 (m), 700 (m), 601 (w), 552 (m), 517 (s). $C_{56}H_{74}Ce_2N_4O_{10}$ (1243.48): calcd. C 54.09, H 6.00, N 4.50; found C 54.51, H 6.39, N 4.31.

$[Ce(DIP)(\mu\text{-}OPc)(\mu_c\text{-}OPc)(py)_2]_2$ (10): Used compound **5** (0.26 g, 0.29 mmol), H-OPc (0.052 g, 0.58 mmol) in py. Yield: 60% (0.12 g). FT-IR (KBr, cm^{-1}): $\tilde{\nu}$ = 3062 (s), 3036 (s), 2968 (w), 2930 (m), 2870 (m), 1581 (w), 1477 (w), 1442 (w), 1422 (w), 1373 (m), 1359 (s), 1283 (w), 1263 (m), 1238 (s), 1217 (s), 1092 (m), 1035 (m), 1004 (s), 850 (m), 753 (m), 702 (m), 619 (s), 547 (s), 531 (s), 518 (s). $C_{60}H_{82}Ce_2N_4O_{10}$ (1299.58): calcd. C 55.45, H 6.36, N 4.31; found C 55.90, H 6.81, N 4.33.

General X-ray Crystal Structure Information:[70] Each crystal was mounted onto a thin glass fiber from a pool of Fluorolube™ and immediately placed under a liquid N_2 stream, on a Bruker AXS diffractometer. The radiation used was graphite-monochromatized Mo-K_α radiation (λ = 0.7107 Å). The lattice parameters were optimized from a least-squares calculation on carefully centered reflections. Lattice parameter determination and data collection were carried out using SMART Version 5.054 software. Data reduction was performed using SAINT Version 6.01 software. The structure refinement was performed using XSHELL 3.0 software. The data were corrected for absorption using the SADABS program within the SAINT software package. General collection parameters for **1**–**3** and **4**–**10** are shown in Table 1 and Table 2, respectively. Additional information concerning the structure of these compounds can be found by accessing the final CIF files through the Cambridge Crystallographic Data Base. In general, each structure was solved by direct methods. This procedure yielded the heavy atoms,

Table 1. Data collection parameters for **1**–**3**.

Compound	**1(·8tol)**	**2**	**2a(·2tol)**	**3(·3THF)**
Empirical formula	$C_{116}H_{196}Ce_4O_{12}$	$C_{48}H_{108}Ce_4O_{12}$	$C_{58}H_{115}Ce_3O_{11}$	$C_{54}H_{87}CeO_9$
Formula weight	2343.32	1437.82	1408.92	1020.36
Temp. [K]	168(2)	168(2)	178(2)	168(2)
Space group	tetragonal	monoclinic	monoclinic	rhombohedral
	P-42(1)c	*P*21/*c*	*P*2(1)	*R*-3
a [Å]	20.5590(18)	18.673(12)	14.1032(17)	14.663(2)
b [Å]	20.5590(18)	11.382(7)	18.952(2)	14.663(2)
c [Å]	11.908(2)	29.308(18)	14.5646(17)	14.663(2)
α [°]				68.220(3)
β [°]		91.335(15)	115.902(2)	68.220(3)
γ [°]				68.220(3)
V [Å^3]	5033.1(11)	6227(7)	3501.7(7)	2617.3(6)
Z	2	4	2	2
D_{calcd} [Mg/m^3]	1.060	1.534	1.336	1.295
μ (Mo-K_α) [mm^{-1}]	1.838	2.917	1.965	0.922
R_1[a] (%) (all data)	7.78 (22.60)	8.55 (16.70)	7.23 (11.87)	4.23 (9.60)
wR_2[b] (%) (all data)	12.30 (25.05)	17.00 (19.94)	11.09 (13.25)	5.90 (9.83)

[a] $R_1 = \Sigma||F_o|-|F_c||/\Sigma|F_o| \times 100$. [b] $wR_2 = [\Sigma w(F_o^2-F_c^2)^2/\Sigma(w|F_o|^2)^2]^{1/2} \times 100$.

Table 2. Data collection parameters for **4**–**10**.

Compound	**4(·2THF)**	**4a(·2tol)**	**5(·tol)**	**6(·2THF)**
Empirical formula	$C_{72}H_{100}Ce_2O_{12}$	$C_{82}H_{90}Ce_2N_4O_6$	$C_{55}H_{83}CeO_6$	$C_{70}H_{71}CeO_7$
Formula weight	1439.78	1507.82	980.33	1164.45
Temp. [K]	168(2)	178(2)	178(2)	203(2)
Space group	monoclinic	monoclinic	monoclinic	monoclinic
	*P*21/*c*	*P*21/*n*	*P*21/*n*	*P*2(1)
a [Å]	12.748(2)	14.600(3)	11.1537(16)	10.220(2)
b [Å]	18.883(3)	19.504(4)	35.671(5)	21.968(5)
c [Å]	15.343(3)	14.690(3)	13.4253(19)	13.461(3)
α [°]				
β [°]	112.723(3)	118.254(2)	96.293(3)	101.110(4)
γ [°]				
V [Å^3]	3406.6(11)	3684.7(11)	5309.2(13)	2965.4(11)
Z	2	2	4	2
D_{calcd} [Mg/m^3]	1.404	1.359	1.226	1.143
μ (Mo-K_α) [mm^{-1}]	1.379	1.274	0.903	0.810
R_1[a] (%) (all data)	3.40 (8.51)	2.74 (6.75)	7.49 (14.48)	4.51 (8.54)
wR_2[b] (%) (all data)	4.07 (8.90)	3.15 (6.97)	13.89 (17.16)	5.51 (8.96)
Compound	**7(·py)**	**8**	**9**	**10(·2py)**
Empirical formula	$C_{65}H_{87}Ce_2N_5O_{10}$	$C_{52}H_{66}Ce_2N_4O_{10}$	$C_{56}H_{74}Ce_2N_4O_{10}$	$C_{70}H_{92}Ce_2N_6O_{10}$
Formula weight	1391.36	1187.33	1243.43	1457.74
Temp. [K]	203(2)	168(2)	178(2)	168(2)
Space group	monoclinic	monoclinic	triclinic	monoclinic
	*P*21/*n*	*C*2/*c*	*P*$\bar{1}$	*P*21/*c*
a [Å]	11.660(3)	20.9692(13)	11.8503(16)	9.883(3)
b [Å]	15.714(5)	13.4977(13)	11.9179(16)	20.157(7)
c [Å]	19.113(6)	20.1132(14)	12.9071(17)	18.208(6)
α [°]			86.896(2)	
β [°]	99.253(5)	107.972(2)	65.609(2)	103.471(7)
γ [°]			65.482(2)	
V [Å^3]	3456.5(17)	5415.0(7)	1495.3(3)	3528(2)
Z	2	4	1	2
D_{calcd} [Mg/m^3]	1.337	1.456	1.381	1.372
μ (Mo-K_α) [mm^{-1}]	1.358	1.717	1.558	1.333
R_1[a] (%) (all data)	8.96 (22.76)	3.82 (10.01)	4.38 (8.37)	7.76 (12.19)
wR_2[b] (%) (all data)	9.80 (23.07)	4.34 (10.30)	5.63 (8.81)	13.50 (13.95)

[a] $R_1 = \Sigma \; | \; |F_o|-|F_c| \; | / \Sigma \; |F_o| \times 100$. [b] $wR_2 = [\Sigma \; w \; (F_o^2-F_c^2)^2/\Sigma \; (w \; |F_o|^2)^2]^{1/2} \times 100$.

along with a number of the C, O, and N atoms when present. Subsequent Fourier synthesis yielded the remaining atom positions. The hydrogen atoms were fixed in positions of ideal geometry and refined within the XSHELL software. These idealized hydrogen atoms had their isotropic temperature factors fixed at 1.2 or 1.5 times the equivalent isotropic *U* of the C atoms to which they were bonded. The final refinement of each compound included anisotropic thermal parameters on all non-hydrogen atoms. Final crystal solutions that contain alkoxides are well known to possess ligand positional disorder issues.

CCDC-614454 to -614465 contain the supplementary crystallographic data for this paper. These data can be obtained free of charge from The Cambridge Crystallographic Data Centre via www.ccdc.cam.ac.uk/data_request/cif. Any variations from standard structural solution associated with the representative compounds are discussed below. All CIF files were checked for errors using the free on-line Checkcif service provided by the International Union of Crystallography (available on the Web at http://checkcif.iucr.org/).

Acknowledgments

For support of this research, the authors would like to thank the Office of Basic Energy Sciences of the Department of Energy and the United States Department of Energy. Sandia is a multiprogram laboratory operated by Sandia Corporation, a Lockheed Martin Company, for the United States Department of Energy under contract DE-AC04-94AL85000.

[1] T. J. Boyle, R. P. Tyner, T. M. Alam, B. L. Scott, J. W. Ziller, B. G. J. Potter, *J. Am. Chem. Soc.* **1999**, *121*, 12104.
[2] T. J. Boyle, L. A. Ottley, M. A. Rodriguez, *Polyhedron* **2005**, *24*, 1727.
[3] S. N. Jacobsen, L. D. Madsen, U. Kelmersson, *J. Mater. Res.* **1999**, *14*, 2385.
[4] M. A. Arranz, B. Holzapfel, N. Reger, J. Eickemeyer, L. Schultz, *Physica C* **2002**, *266*, 109.
[5] C. S. Oh, C. I. Kim, K. H. Kwon, *J. Vac. Sci. Technol.* **2001**, *19*, 1068.
[6] R. Reisfeld, M. Zayat, H. Minti, A. Zastrow, *Sol. Energy Mater. Sol. Cells* **1998**, *54*, 109.
[7] G. S. Qi, R. T. Yang, R. Chang, *Appl. Catal., B* **2004**, *51*, 93.
[8] K. Tomishige, M. Asadullah, K. Kunimori, *Catal. Today* **2004**, *89*, 389.
[9] C. H. Wang, S. S. Lin, *Appl Catal., A* **2004**, *268*, 227.
[10] N. Kakuta, H. Ohkita, T. Mizushima, *J. Rare Earths* **2004**, *22*, 1.
[11] X. M. Qi, M. Flytzani-Stephanopoulos, *Ind. Eng. Chem. Res.* **2004**, *43*, 3055.
[12] J. Soler, T. Gonzalez, M. J. Escudero, T. Rodrigo, L. Daza, *J. Power Sources* **2002**, *106*, 189.
[13] C. Hatchwell, N. M. Sammes, I. W. M. Brown, *Solid State Ionics* **1999**, *126*, 201.
[14] A. Atkinson, *Solid State Ionics* **1997**, *95*, 249.
[15] R. Sabia, H. J. Stevens, *Machining Sci. Technol.* **2000**, *4*, 235.
[16] B. K. Tanner, T. P. A. Hase, H. Z. Wu, *Philos. Magn. Lett.* **2001**, *81*, 351.
[17] G. B. Deacon, T. C. Feng, C. M. Forsyth, A. Gitlits, D. C. R. Hockless, S. Qi, B. W. Skelton, A. H. White, *J. Chem. Soc., Dalton Trans.* **2000**, 961–966.
[18] W. J. Evans, T. J. Deming, J. M. Olofson, J. W. Ziller, *Inorg. Chem.* **1989**, *28*, 4027.
[19] P. S. Gradeff, K. Yunlu, T. J. Deming, J. M. Olofson, *Inorg. Chem.* **1990**, *29*, 420.
[20] Y. K. Gun'ko, S. D. Elliott, P. B. Hitchcock, M. F. Lappert, *J. Chem. Soc., Dalton Trans.* **2002**, 1852.
[21] L. G. Hubert-Pfalzgraf, N. El Khokh, J.-C. Daran, *Polyhedron* **1992**, *11*, 59.
[22] A. Sen, A. L. Rheingold, M. B. Allen, *Private Communication with Cambridge Data Base* **1996**.
[23] A. Sen, H. A. Stecher, A. L. Rheingold, *Inorg. Chem.* **1992**, *31*, 473.
[24] C. Sirio, L. G. Hubert-Pfalzgraf, C. Bois, *Polyhedron* **1997**, *16*, 1129.
[25] H. A. Stecher, A. Sen, A. L. Rheingold, *Inorg. Chem.* **1988**, *27*, 1130–1132.
[26] H. A. Stecher, A. Sen, A. L. Rheingold, *Inorg. Chem.* **1989**, *28*, 3280.
[27] P. Tolendao, F. Ribot, C. Sanchez, *Acta Crystallogr., Sect. C* **1990**, *46*, 1419.
[28] B. A. Vaarstrstra, J. C. Huffman, P. S. Gradeeff, L. G. Hubert-Pfalzgraf, J. C. Daran, S. Parraud, K. Yunlu, K. G. Caulton, *Inorg. Chem.* **1990**, *29*, 3126.
[29] K. Yunlu, P. S. Gradeff, N. Edelstein, W. Kot, G. Shalimoff, W. E. Steib, B. A. Vaartstra, K. G. Caulton, *Inorg. Chem.* **1991**, *30*, 2317–2321.
[30] L. G. Hubert-Pfalzgraf, V. Abada, J. Vaissermann, *Polyhedron* **1999**, *8*, 3497.
[31] L. G. Hubert-Pfalzgraf, C. Sirio, C. Bois, *Polyhedron* **1998**, *17*, 821.
[32] T. J. Boyle, S. D. Bunge, P. G. Clem, J. Richardson, J. T. Dawley, L. A. M. Ottley, M. A. Rodriguez, B. A. Tuttle, G. Avilucea, R. G. Tissot, *Inorg. Chem.* **2005**, *44*, 1588.
[33] T. J. Boyle, L. A. M. Ottley, L. J. Tribby, S. D. Bunge, C. J. Gordon, *Chem. Mater.* **2005**, (*in preparation*).
[34] D. M. Barnhart, D. L. Clark, J. C. Gordon, J. C. Huffman, J. G. Watkin, B. D. Zwick, *J. Am. Chem. Soc.* **1993**, *115*, 8461.
[35] D. C. Bradley, R. C. Mehrotra, D. P. Gaur, *Metal Alkoxides*, Academic Press, New York, **1978**.
[36] D. C. Bradley, R. C. Mehrotra, I. P. Rothwell and A. Singh, *Alkoxo and Aryloxo Derivatives of Metals*, Academic Press, New York, **2001**, p. 704.
[37] T. J. Boyle, S. D. Bunge, P. G. Clem, J. Richardson, J. T. Dawley, L. A. M. Ottley, M. A. Rodriguez, B. A. Tuttle, G. R. Avilucea, R. G. Tissot, *Inorg. Chem.* **2005**, *44*, 1588.
[38] W. J. Evans, R. E. Golden, J. W. Ziller, *Inorg. Chem.* **1993**, *32*, 3041.
[39] W. J. Evans, M. A. Ansari, J. W. Ziller, *Polyhedron* **1997**, *16*, 3429.
[40] The database of The Cambridge Crystallographic Data Centre, 12 Union Road, Cambridge CB2 1EZ, United Kingdom, www.ccdc.cam.ac.uk, was searched using ConQuest v 5.27 (Jan. **2006**).
[41] W. J. Evans, J. M. Olofson, J. W. Ziller, *Inorg. Chem.* **1989**, *28*, 4308–4309.
[42] G. B. Deacon, F. Tiecheng, B. W. Skelton, A. H. White, *Aust. J. Chem.* **1995**, *48*, 741.
[43] Z. Xie, K. Chui, Q. Yang, T. C. W. Mak, J. Sun, *Organometallics* **1998**, *17*, 3937.
[44] G. B. Deacon, B. M. Gatehouse, Q. Shen, G. N. Ward, E. R. T. Tiekink, *Polyhedron* **1993**, *12*, 1289.
[45] G. B. Deacon, S. Nickel, P. Mackinnon, E. R. T. Tiekink, *Aust. J. Chem.* **1990**, *43*, 1245.
[46] G. B. Deacon, F. Tiecheng, S. Nickel, M. I. Ogden, A. H. White, *Aust. J. Chem.* **1992**, *45*, 671.
[47] D. M. Barnhart, D. L. Clark, J. C. Gordon, J. C. Huffman, R. L. Vincent-Hollis, J. G. Watkin, B. D. Zwick, *Inorg. Chem.* **1994**, *33*, 3487.
[48] S. Suh, J. Guan, L. A. Miinea, J.-S. M. Lehn, *Chem. Mater.* **2004**, *16*, 1667.
[49] D. C. Bradley, H. Chudzynska, M. B. Hursthouse, M. Motevalli, *Polyhedron* **1991**, *10*, 1049–1059.
[50] T. J. Boyle, N. L. Andrews, T. A. Alam, M. A. Rodriguez, J. M. Santana, B. L. Scott, *Polyhedron* **2002**, *21*, 2333.
[51] T. J. Boyle, T. A. Alam, C. J. Tafoya, B. L. Scott, *Inorg. Chem.* **1998**, *37*, 5588.
[52] W. Brzysk, Z. Rzaczynska, E. Swita, R. Mrozek, T. Glowiak, *J. Coord. Chem.* **1997**, *41*, 1.
[53] U. Baish, D. B. Dell'Amico, F. Calderazzo, L. Labella, *J. Mol. Catal. A* **2003**, *204*, 259.
[54] P. C. Junk, C. J. Kepert, W. M. Lu, B. W. Skelton, A. H. White, *Aust. J. Chem.* **1999**, *52*, 437–457.
[55] Z. Long-Guan, Y. Qing-Sen, X. Xue-Peng, *Jiegou Huaxue (Chin.) Chinese J. Struct. Chem.* **1998**, *17*, 281.
[56] C.-Y. Xian, L.-G. Zhu, Q.-S. Yu, *Wuji Huaxue Xuebao (Chin.)* **1999**, *15*, 813.

[57] S.-H. Zhao, C.-Y. Xian, *Wuji Huaxue Xuebao (Chin.)* **2002**, *18*, 639.
[58] A. Panagiotopoulos, T. F. Zafiropopulos, S. P. Perlepes, E. Bakalbassis, I. Masson-Ramade, O. Kahn, A. Terzis, C. P. Raptopoulou, *Inorg. Chem.* **1995**, *34*, 4918.
[59] L.-Z. Cai, W.-T. Chen, M.-S. Wang, G.-G. Guo, J.-S. Huang, *Inorg. Chem. Commun.* **2004**, *7*, 611.
[60] B. Wu, Y.-S. Guo, *Acta Crystallogr., Sect E. Struct. Rep. Onlin Sect. E* **2004**, *60*, m1261.
[61] A.-Y. Fu, S.-Z. Fu, T. Yu, *Acta Crystallogr., Sect E. Struct. Rep. Onlin Sect. E* **2005**, *61*, m223.
[62] L.-L. Wen, B.-G. Zhang, Z.-H. Peng, *Wuji Huaxue Xuebao (Chin.)* **2004**, *20*, 1228.
[63] F. A. Cotton and G. Wilkinson, *Advanced Inorganic Chemistry, Fifth Edition*, John Wiley & Sons, New York, **1988**, p.
[64] T. J. Boyle, L. A. M. Ottley, M. A. Rodriguez, *Polyhedron* **2005**, *24*, 1727.
[65] T. J. Boyle, N. L. Andrews, T. M. Alam, M. A. Rodriguez, J. M. Santana, B. L. Scott, *Polyhedron* **2002**, *21*, 2333.
[66] T. J. Boyle, N. L. Andrews, M. A. Rodriguez, C. Campana, T. Yiu, *Inorg. Chem.* **2003**, *42*, 5357.
[67] T. J. Boyle, D. M. Pedrotty, T. M. Alam, S. C. Vick, M. A. Rodriguez, *Inorg. Chem.* **2000**, *39*, 5133–5146.
[68] G. B. Deacon, R. J. Phillips, *Coord. Chem. Rev.* **1980**, *33*, 227–250.
[69] D. D. Perrin and W. L. F. Armarego, *Purification of Laboratory Chemicals*, Pergamon Press, New York, **1988**, p.
[70] The listed versions of SAINT, SMART, XSHELL, XPOW in SHELXTL, and SADABS software from Bruker Analytical X-ray Systems Inc., 6300 Enterprise Lane, Madison, WI 53719 were used in the analysis.

Received: June 29, 2006
Published Online: September 20, 2006

